

# *In situ* diffuse reflectance IR spectroscopy and X-ray absorption spectroscopy for fast catalytic processes

Nebojsa S. Marinkovic,<sup>a\*</sup> Qi Wang<sup>a\*</sup> and Anatoly I. Frenkel<sup>b\*</sup>

Received 17 December 2010

Accepted 16 February 2011

<sup>a</sup>Synchrotron Catalysis Consortium, University of Delaware, 150 Academy St, Newark, DE 19716, USA, and <sup>b</sup>Physics Department, Yeshiva University, New York, NY 10016, USA.

E-mail: marinkov@bnl.gov, qwang@bnl.gov, anatoly.frenkel@yu.edu

A new instrument for synchronous *in situ* investigations of catalytic materials by IR and X-ray absorption spectroscopies was designed and built at the X18A beamline of the National Synchrotron Light Source of Brookhaven National Laboratory. It provides analytical tools for solving structural, electronic and kinetic problems in catalysis science by two complementary methods. Among the features attractive for catalysis research are the broad range of catalytically active elements that can be investigated (starting with Ni and beyond), the wide range of reaction conditions (temperatures up to 873 K, various reactive gases) and time scales (starting from tens of seconds). The results of several representative experiments that illustrate the attractive capabilities of the new set-up are discussed.

© 2011 International Union of Crystallography  
Printed in Singapore – all rights reserved**Keywords:** diffuse reflectance IR spectroscopy; catalysis science; X-ray absorption spectroscopy; scattering techniques.

## 1. Introduction

Many physical and chemical processes, in particular chemical reactions, need to be studied *in situ* in order to follow the reaction pathways and understand the mechanisms of transformations (Somorjai & Aliaga, 2010; Weckhuysen, 2002). *In situ* studies of the reactivity of nanocatalysts are particularly challenging as they require a combination of several complementary techniques in a single experiment (Brückner, 2001; Grunwaldt & Clausen, 2002; Newton *et al.*, 2004; Beale & Sankar, 2002). Studies of many catalytic processes by synchrotron X-ray absorption and scattering techniques combined in a single experiment, as an example (Clausen & Topsoe, 1994; Clausen, 1998; Clausen *et al.*, 1998), have been particularly insightful as they provide access to multiple length scales important for catalysis: the nanometer scale for the description of nanoparticles, and the micrometer scale for description of the support materials. Raman and infrared (IR) spectroscopies provide a unique opportunity to understand the interactions of catalysts and reactants, and these techniques have been successfully integrated with X-ray methods for *in situ* investigations (Grundwalt & Baiker, 2005; Newton *et al.*, 2007; Tinnemans *et al.*, 2006).

In this work we describe the new tools for combined use of X-ray absorption spectroscopy and IR spectroscopy techniques for fast (with sub-second time resolution) studies of nanocatalysts, optimized for *in situ* experiments. These techniques provide complementary information about chemical transformations in the sample, and help shed light on the role that catalysts play in them. X-ray absorption spectroscopy

(XAS), through its two modifications, extended X-ray absorption fine structure (EXAFS) and X-ray absorption near-edge structure (XANES), investigates the catalyst structure and electronic state, and monitors their changes during the reaction. Advances in X-ray instrumentation, namely, dispersive EXAFS (Hagelstein *et al.*, 1995) and Quick EXAFS (QEXAFS; Frahm, 1989; Khalid *et al.*, 2010) techniques, allow studying real-time processes with a time resolution of tens of milliseconds. New data analysis methods (Frenkel *et al.*, 2002; Wang *et al.*, 2008) were developed to study rapid reaction kinetics investigated by these X-ray techniques.

EXAFS and XANES are not particularly efficient techniques for studies of the surface structure of nanoparticle catalysts during their interactions with reactants, *e.g.* adsorbates and ligands attached to the catalyst surface, because their signal is dominated by the absorber atoms inside the nanoparticles. Diffuse-reflectance IR Fourier-transform spectroscopy (DRIFTS) is a unique alternative for such analysis due to the sensitivity on the atomic groups adsorbed on the surface of the catalyst. The latter technique gives details on the chemical structure of the active centers of the catalyst in addition to obvious gas-phase characterization, and can be used even if the sample is opaque for the transmission IR measurements (Benitez *et al.*, 1993) while having a large penetration depth in comparison with other IR techniques (Griffiths & de Haseth, 2007). Furthermore, unlike transmission IR that usually requires a pressed wafer for the measurement (which limits its usefulness for the *in situ* gas catalysis investigation because of diffusion problems), the DRIFTS technique analyzes powder surfaces. *In situ* char-

acterization of surface composition, reaction mechanisms and pathways, and identification of the reaction intermediates are successfully performed using this technique, especially if it is coupled with residual gas analysis (mass spectrometry or gas chromatography).

The power of DRIFTS and XAS as separate techniques for characterization of catalytic surfaces has been previously demonstrated (Lu *et al.*, 2008; Klasovsky *et al.*, 2008). Newton *et al.* combined these techniques in the *in situ* synchrotron experiment and showed, for the first time, that the changes in the catalyst structure correlate with metal–adsorbate interactions (Newton *et al.*, 2007a,b; Newton, Belver-Coldeira *et al.*, 2007; Newton, 2009).

In this article we present a new suite of instruments for combining DRIFTS with XAFS, complemented by mass-spectrometric residual gas analysis (RGA; Estrella *et al.*, 2009). These instruments provide access to a broad energy range in both X-ray and IR regimes, as well as the wide temperature range and the time resolution in the seconds range. The new set-up is available at the beamline X18A of the National Synchrotron Light Source (NSLS), Brookhaven National Laboratory in Upton, NY, USA.

### 2. The XAS–DRIFTS set-up

Bending-magnet beamline X18A at the National Synchrotron Light Source has been recently upgraded with an energy-scanning monochromator and QEXAFS capability. Located at 10.1 m from the source, the monochromator uses a Si (111) channel-cut crystal and enables the energy range 5–40 keV. It can be driven by a stepping motor to scan the energy at a standard speed for regular XAFS (several minutes per scan). Alternatively, it can be driven through a given energy range with a tangential arm at 0.1–1.2 Hz frequency using an exocentric cam and a DC motor to perform QEXAFS. The angle of the monochromator crystal is read independently by an optical encoder (Heidenhain). A rhodium-coated toroidal focusing mirror located 11.75 m from the source provides a 0.75 mm (horizontal) × 0.75 mm (vertical) spot size at the sample position, with a flux of  $\sim 2.5 \times 10^{11}$  photons  $s^{-1}$  at 10 keV. Various choices of cams, each featured with a different angular range (0.1, 0.2, 0.5, 1, 2 and 5°) for the monochromator are available for energy scans in QEXAFS mode. The data collection is performed using custom-designed software (So *et al.*, 2007). The current version of the data acquisition program reads the data in cycles of 30 s and 2000 data points  $s^{-1}$ . Presently, one full XANES or EXAFS scan can be completed in 0.4 s at the X18A beamline. While a single scan can produce an XAS spectrum with sufficient signal-to-noise ratio when the concentration of the absorbing metal is high, as in metal foil (Khalid *et al.*, 2010), for real catalysts with metal loading of a few weight percent it is necessary to average many scans. Typically, a good quality average spectrum is obtained after merging the scans over 5–10 s (Khalid *et al.*, 2010).

The instrument for collecting combined XAS and DRIFTS data consists of an IR spectrometer and a prototype of external DRIFTS accessory. The IR spectrometer, Thermo-

Nicolet 6700 (<http://www.thermoscientific.com/>) is equipped with two beamsplitters (KBr and solid substrate) for scanning in mid- and far-IR modes, respectively. Two rapid-scanning liquid-nitrogen-cooled mercury cadmium telluride (MCT) detectors are available for scanning in mid-IR range. The MCT-A detector operates in the frequency range 4000–600  $cm^{-1}$  and has about ten times greater sensitivity than the MCT-B detector. The latter detector offers a somewhat larger operating frequency range (7400–400  $cm^{-1}$ ) than that of MCT-A. For a quick check of the sample and when rapid scanning is not needed, a deuterated lanthanum triglycine sulfate (DLaTGS) detector with KBr window (7400–350  $cm^{-1}$ ) is used because this detector requires no special pretreatment to run. In the far-IR range the solid-state beamsplitter is paired with a DLaTGS detector with a polyethylene window to cover the energy range 700–50  $cm^{-1}$ . The spectrometer has room for two detectors in its detector chamber and a mirror directs the IR light to the detector of choice. Beamsplitters are quickly interchangeable (*i.e.* plug and play) without the need to open the spectrometer. Two thin windows separate the spectrometer's sample chamber from its internal optics, and the interior of the spectrometer is constantly purged with dry nitrogen supplied from the liquid-nitrogen Dewar.

The DRIFTS set-up is assembled from Harrick accessories (<http://www.harricksci.com/>) and consists of a DaVinci arm attached to a modified Praying Mantis DRIFTS accessory, and a modified reaction cell (Fig. 1). The entire assembly is firmly attached to the internal sample chamber of the Nicolet spectrometer. The DaVinci arm redirects the IR beam to

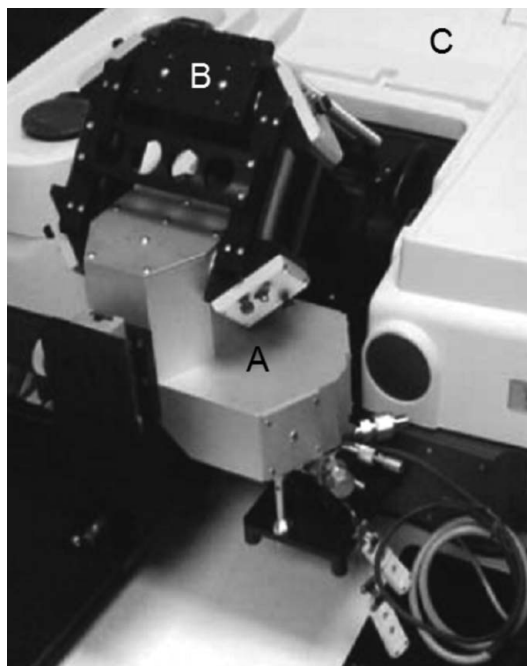


**Figure 1** XAS/DRIFTS set-up consisting of (A) Harrick Praying Mantis, (B) Harrick DaVinci arm and (C) Nicolet 6700 IR spectrometer. A Harrick reaction chamber (see Fig. 2) is inserted into the Praying Mantis from the bottom.

the reaction cell located outside the spectrometer. This spatial arrangement is required to accommodate an X-ray beam path through the chamber. One of two ellipsoids inside the Praying Mantis focuses the IR light on the sample, while the other captures diffusely reflected light; the diffusely reflected light is then sent back to the spectrometer through the DaVinci arm and focused onto one of the IR detectors in the spectrometer.<sup>1</sup> By azimuthally tilting the angle of the ellipsoidal mirrors to 120°, the Praying Mantis DRIFTS design effectively removes specular reflection, allowing only diffuse reflected light to reach the detector. The entire optical path of the XAS/DRIFTS instrument is purged with dry nitrogen to remove water vapor and carbon dioxide that would otherwise mask a large portion of the IR spectrum. In rapid scanning mode the instrument produces a good quality DRIFTS spectrum in about 10 s.

The spectrometer with the XAS/DRIFTS accessory is firmly attached onto a custom-made table that provides precise alignment of the sample to the X-ray beam by means of the five independently driven computer-controlled motors. Three motors lift and tilt the table vertically, the fourth motor adjusts the horizontal position (perpendicular to the beam), and the fifth motor pivots and rotates the table about the vertical axis that passes through the sample. Two gas-filled ion chambers measure the intensity of the X-ray beam before and after the sample (incident beam detector  $I_0$  and transmission detector  $I_t$ ). Another ion chamber (reference detector  $I_{ref}$ ), positioned downstream of the transmission detector, measures the beam intensity through a reference sample (e.g. a metal foil) for X-ray energy calibration.

The reaction chamber is shown in Fig. 2. Two KBr windows positioned at  $\sim 45^\circ$  from each other are installed on a hemispherical shape of stainless steel dome to allow the passage of IR light. Near the bottom of the dome, two smaller glassy carbon windows (1.7 mm in diameter) allow the passage of the X-ray beam. The body of the reaction chamber has an internal volume of  $\sim 14$  ml. It contains three connections for gas purge. Depending on whether the gas blankets the powdered sample or flows through it, different inlet connections are used. In the test experiments described in this article, only the mode where the gas flew through the catalyst was used. Additional

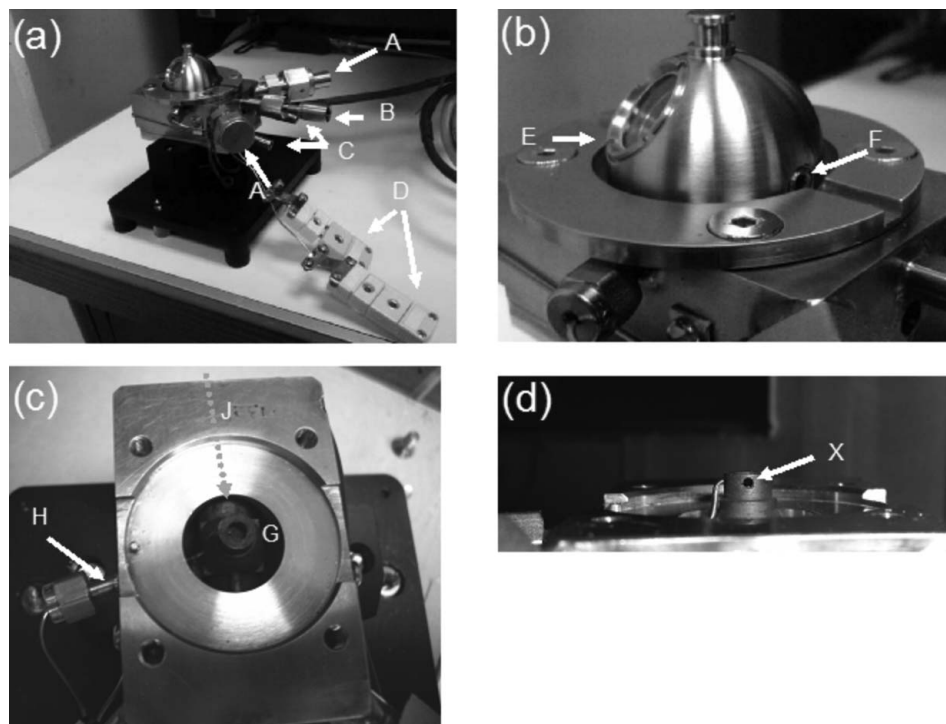


**Figure 2**

Photographs of (a) the assembled Harrick high-temperature reaction chamber, showing the connections for gas flow (A and B), cooling water (C) and thermocouples (D); (b) close-up of the high-temperature reaction chamber dome with windows for the IR light (E) and X-ray light (F); (c) dome interior, showing the XAS/DRIFTS sample cup (G), thermocouple connector (H) and the X-ray path (J); (d) side view of the sample cup with the hole for X-rays (X). Two modes of gas flow are possible: (i) when B is closed the gas flows over the surface of the catalyst, and (ii) when one of the A connections is closed the gas flows through the catalyst bed.

connectors include the input and output for cooling water, a temperature controller connection and two thermocouples, one for the sample temperature and the other for the over-temperature control (Fig. 2a). The sample can be thermally treated over a wide range of temperatures (123–874 K in vacuum, or up to 773 K at atmospheric pressure).

The powdered sample is loaded in a stainless steel cup in the middle of the reaction chamber (Fig. 2b). The total volume of the sample cup is 21.5 mm<sup>3</sup>. The sample cup of the reaction chamber has an inner diameter of 3.17 mm which accommodates well the IR focal spot size on the sample. The X-ray beam traverses through two circular openings in the sample cup, the central axis of which is located 1.04 mm below the cup's top surface. The closest distance from the sample top surface (i.e. the IR probe area) and the X-ray path is 0.37 mm, i.e. the distance from the top surface to the top of the circular opening [Figs. 2(c) and 2(d)]. We have designed a removable cup with a smaller diameter ( $\sim 2.2$  mm) which can be inserted for studies of elements with lower atomic numbers and thus smaller X-ray absorption lengths. We discuss below the implications of these factors on the results of the *in situ* experiments.

An important question of complementarity of XAS and DRIFTS is that the two techniques collect data through different portions of the sample separated vertically by a few hundreds of micrometers. We note here that the penetration

<sup>1</sup> For detailed schematic please contact the authors.

depth of IR radiation into the sample depends on the optical properties of the sample. The penetration depth of the IR beam can reach 3 mm (Griffiths & de Haseth, 2007) in non-absorbing diluting powders (*e.g.* KBr or  $\text{Al}_2\text{O}_3$ ) if no overlayer is used to attenuate it for depth profiling (Fondeur & Mitchell, 2000). Thus, a significant portion of the IR beam samples the same volume through which the X-ray beam traverses. It is, however, unavoidable in such experiments to have some portion of the sample illuminated only by one beam but not the other, as happens, for example, in the horizontal plane, owing to the different shapes of the beam profiles (a circular footprint of the IR beam and the rectangular profile of the X-ray path). Owing to the temperature and compositional gradients, these factors limit the interpretation of the combination of such techniques and special care is needed to estimate them in each experiment.

### 3. Experimental

The assessments of the new instrument were performed both *ex situ*, to characterize the ranges and the performances of individual (DRIFTS and XAS) techniques, and *in situ*, to characterize the complete set-up in the process of measurement of a system undergoing chemical transformations. Both XAS and DRIFTS techniques were used in their normal modes of operation, *i.e.* without quick or rapid scanning.

#### 3.1. *Ex situ* experiments of DRIFTS

Metal-carbonyl complexes are a convenient test IR system as they can be easily monitored through the intense carbonyl vibrations. Fig. 3(a) shows DRIFT spectra of the  $\text{Ru}_3(\text{CO})_{12}$  complex mixed with  $\text{Al}_2\text{O}_3$  (6 wt% Ru), as well as that from  $\text{Al}_2\text{O}_3$ , referenced to the spectra of pure powdered KBr. While the spectrum of alumina contains only a strong broad band around  $1100\text{ cm}^{-1}$ , the spectrum of  $\text{Ru}_3(\text{CO})_{12}$  complex mixed with  $\text{Al}_2\text{O}_3$  shows three strong bands in the  $2000\text{--}2100\text{ cm}^{-1}$  range. A comparison of the frequencies of the bands with

those found in the literature (<http://www.sigmaaldrich.com/spectra/ftir/FTIR003760.PDF>) for the pure  $\text{Ru}_3(\text{CO})_{12}$  compound shows a close match. However, the relative intensities of the bands differ somewhat. The literature spectrum of  $\text{Ru}_3(\text{CO})_{12}$  shows two strong bands at  $2060$  and  $2030\text{ cm}^{-1}$ , a medium-intensity band around  $2000\text{ cm}^{-1}$  and two weak bands around  $2130$  and  $1950\text{ cm}^{-1}$ . It was shown that the bands vary both in intensity and frequency, depending on support and exposure to air (Goodwin & Naccache, 1982). It is important to note that the literature spectrum provided by Sigma-Aldrich is taken in transmission mode which is often regarded as a more sensitive technique than DRIFTS. However, the two techniques are guided with different absorption principles and their sensitivity can be only compared by the observed band intensities (Fuller & Griffiths, 1980). The ability to observe even the weakest bands in Fig. 3(a) attests to a good sensitivity and alignment of our DRIFTS accessory.

Typical working catalysts rarely have metal loading above 5 wt%. Since the spectrum given in Fig. 3(a) contains 6 wt% Ru, a separate test was needed to explore the sensitivity of the combined XAS/DRIFTS set-up with metal loadings closer to those of real catalysts. Fig. 3(b) shows a DRIFTS spectrum of carbonyl adsorbates formed on  $\text{Pt}/\gamma\text{-Al}_2\text{O}_3$  in reaction with gaseous CO. The sample was prepared by the impregnation method, resulting in the Pt loading of 1 wt%. The Pt surface was first reduced in a stream of 5%  $\text{H}_2/\text{He}$  at 673 K. After replacing the gas with He to remove traces of hydrogen, a 5% CO in He mixture was flown through the powder catalyst and DRIFTS spectra were recorded. The DRIFTS spectrum shows two strong bands at  $2180$  and  $2120\text{ cm}^{-1}$  and a shoulder around  $2060\text{ cm}^{-1}$ . The two former bands are characteristic of gaseous CO, while the shoulder is believed to be a carbonyl feature owing to CO bonded linearly to metallic Pt. The signal quality suggests that detection of the metal-carbonyl interaction is possible at the metal loading being as low as 1%, and that our system has a high sensitivity for catalysts under *in situ* conditions.

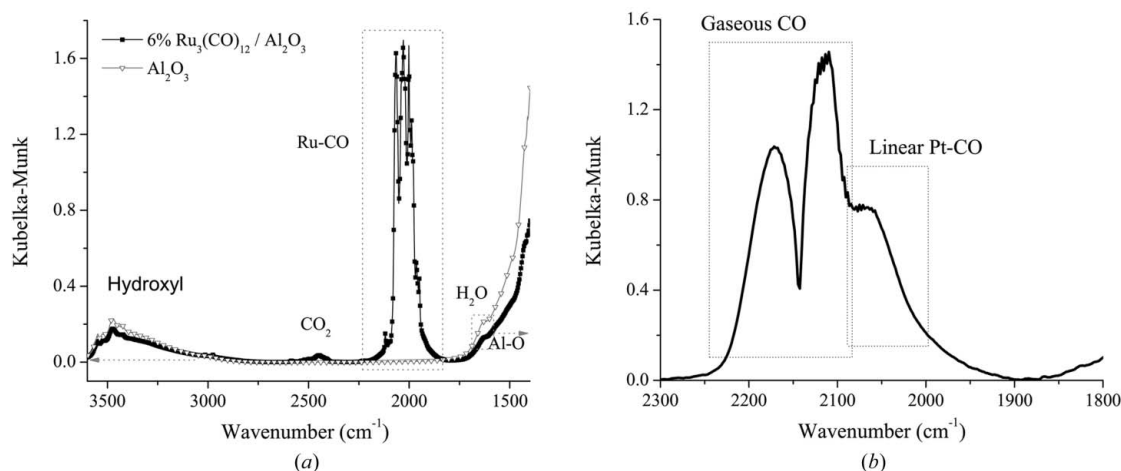


**Figure 3**

(a) IR spectra of 6 wt%  $\text{Ru}_3(\text{CO})_{12}$  in  $\text{Al}_2\text{O}_3$  (black line) and pure  $\text{Al}_2\text{O}_3$  (gray); (b) CO absorption on 1 wt%  $\text{Pt}/\text{Al}_2\text{O}_3$ . 128 scans with  $4\text{ cm}^{-1}$  resolution were combined. Reference spectrum is pure KBr powder.

### 3.2. *Ex situ* experiments of XAS capability

Existing combinations of XAS and DRIFTS have been exploited primarily for high-atomic-number elements, such as Pd or Rh (Evans *et al.*, 2007), where the contrast between the absorption by the element and by the matrix (*e.g.*  $\gamma$ -Al<sub>2</sub>O<sub>3</sub>) is large. This requirement is critical for the transmission mode of XAS measurement where a large total absorption owing to the combined thickness of the sample and the matrix degrades the quality of the absorption coefficient signal. This situation is particularly likely to occur in the XAS/DRIFTS chamber where the X-ray beam probes a large sample thickness (of the order of a few millimeters), but no tests have been carried out, to the best of our knowledge, to experimentally find the range of metals and substrates that afford a good condition for combined measurements. Establishing such a range experimentally is important for characterizing the versatility of this system for catalysis research. Toward this goal, we selected three elements: Ni (*K*-edge energy: 8333 eV), Pt (*L*<sub>3</sub>-edge: 11564 eV) and Ru (*K*-edge: 22117 eV) to explore the feasibility of our set-up in different energy regions. All measurements were conducted with a special insert to the reactor cup that limits the path length of X-rays to 2.2 mm. The following two systems were tested by both *ex situ* DRIFTS and *ex situ* XAFS: Ru<sub>3</sub>(CO)<sub>12</sub> complex (6 wt% Ru) and Pt nanoparticles (1 wt%) supported on  $\gamma$ -Al<sub>2</sub>O<sub>3</sub>. In addition, a sample containing Ni nanoparticles (16 wt%) supported on  $\gamma$ -Al<sub>2</sub>O<sub>3</sub> was diluted further to 4 wt% by mixing with  $\gamma$ -Al<sub>2</sub>O<sub>3</sub> powder and then measured by *ex situ* XAFS. All the measurements were carried out in the XAS/DRIFTS chamber with and without the KBr dome, in order to evaluate both the glassy carbon window effect and the chamber feasibility for different energy regions. The data are shown in Fig. 4. Comparable XAFS data qualities were obtained for all cases, regardless of whether the X-ray beam passed through glassy carbon windows or not. Good signal for all edges show that the set-up can be used over a wide range of energies without the loss of sensitivity. We also comment on the good agreement between the data acquired using this XAS/DRIFTS chamber and the spectrum obtained by a conventionally prepared pellet sample. Therefore, we conclude that both XANES and EXAFS data are adequate for quantitative analysis. Also, excellent data quality obtained in a few minutes per scan acquisition time demonstrated that the set-up may be also used for time-resolved measurements, including QEXAFS.

### 3.3. *In situ* experiments in the XAFS/DRIFTS chamber

CO adsorption on Pt/ $\gamma$ -Al<sub>2</sub>O<sub>3</sub> has been tested extensively using IR techniques because the stretching frequency of the band,  $\nu(\text{CO})$ , has a strong extinction coefficient and is sensitive to a number of factors. Two bands are commonly found at CO adsorption on Pt, one around 2050 cm<sup>-1</sup> and the other around 1850 cm<sup>-1</sup>, corresponding to the carbon monoxide adsorbed on a single Pt atom (linearly bonded carbon monoxide CO<sub>L</sub>), and the CO occupying two Pt atoms (bridge-bonded carbon monoxide, CO<sub>B</sub>), respectively. The former

band is known to be more affected by various factors such as the CO coverage (Eichens & Pliskin, 1958; Blyholder, 1964, 1975; Primet *et al.*, 1973), the presence of Lewis acids or electron acceptors concomitantly adsorbed on the metal surface (Blyholder, 1964; Queau & Poilblanc, 1972; Primet, 1984), as well as the nature and oxidation state of the metal and the time and character of the metal pretreatment (Chang & Chang, 1998; Gottschalk *et al.*, 2010). Complementary XAS analysis adds information on the electronic (XANES) and structural (EXAFS) details of metal species that can be affected by either pretreatment or *in situ* processing of the sample. In combination, the XAS/DRIFTS technique is a perfect match for studying such processes simultaneously during *in situ* conditions, in which the IR probes the metal adsorbate interactions described above, whilst XAFS provides complementary information on the structural and electronic properties (*e.g.* oxidation states) of the metal framework.

In the following experiment a commercially available sample of 5% Pt supported on Al<sub>2</sub>O<sub>3</sub> was employed. The powder was loaded in the removable insert sample cup, which in turn was inserted into the reaction chamber. At first the sample was reduced by heating from room temperature to 673 K in the flow of 5% H<sub>2</sub>/He. The reduction of Pt was followed by re-oxidation using 20% O<sub>2</sub>/He. In the second test such a re-oxidized Pt surface was subjected to a 5% CO/He mixture and heated to 473 K, and then temperature was allowed to decrease to room temperature. The experiment was finished by complete adsorption of CO at room temperature, followed by gradual CO desorption at elevated temperatures in the stream of He flow. XAFS/DRIFTS data were acquired continuously during the entire process.

Fig. 5 shows the *in situ* XANES and DRIFT spectra collected during the reduction of Pt/ $\gamma$ -Al<sub>2</sub>O<sub>3</sub> in 5% H<sub>2</sub>/He atmosphere while ramping the temperature from room temperature to 673 K at a rate of 5 K min<sup>-1</sup>. The reduction of Pt particles is clearly evident in the XANES spectra (Fig. 5*b*) by the decrease in the white line intensity (Brown *et al.*, 1977). DRIFT spectra, recorded simultaneously with XAS, are shown in Fig. 5(*a*). Two bands are visible at lower temperatures at 2120 and 2050 cm<sup>-1</sup>. As the temperature changes, the former band weakens in intensity and eventually disappears from the spectrum around 423 K, whereas the lower-frequency band increases in height and shifts in frequency from 2050 to 2060 cm<sup>-1</sup>. The highest intensity and the frequency of the latter band were found at 623 K. A further temperature increase causes the band to decrease in intensity and to shift towards lower wavenumbers. The origin of the higher frequency peak is usually associated with the weak Pt–H vibration, whereas that at 2060 cm<sup>-1</sup> is believed to be caused by CO impurities (Szilagyi, 1990; Liu *et al.*, 2001).

At the next stage we studied the temperature-dependent reduction and CO adsorption of the 5% Pt/ $\gamma$ -Al<sub>2</sub>O<sub>3</sub> catalyst under CO/He flow. Figs. 6(*a*) and 6(*b*) show the DRIFT and X-ray absorption spectra, respectively, collected during the heating of the catalyst in CO from room temperature up to 473 K. The first two spectra in Figs. 6(*a*) and 6(*b*) were taken at room temperature in He, and in 5% CO/He flow. We observed

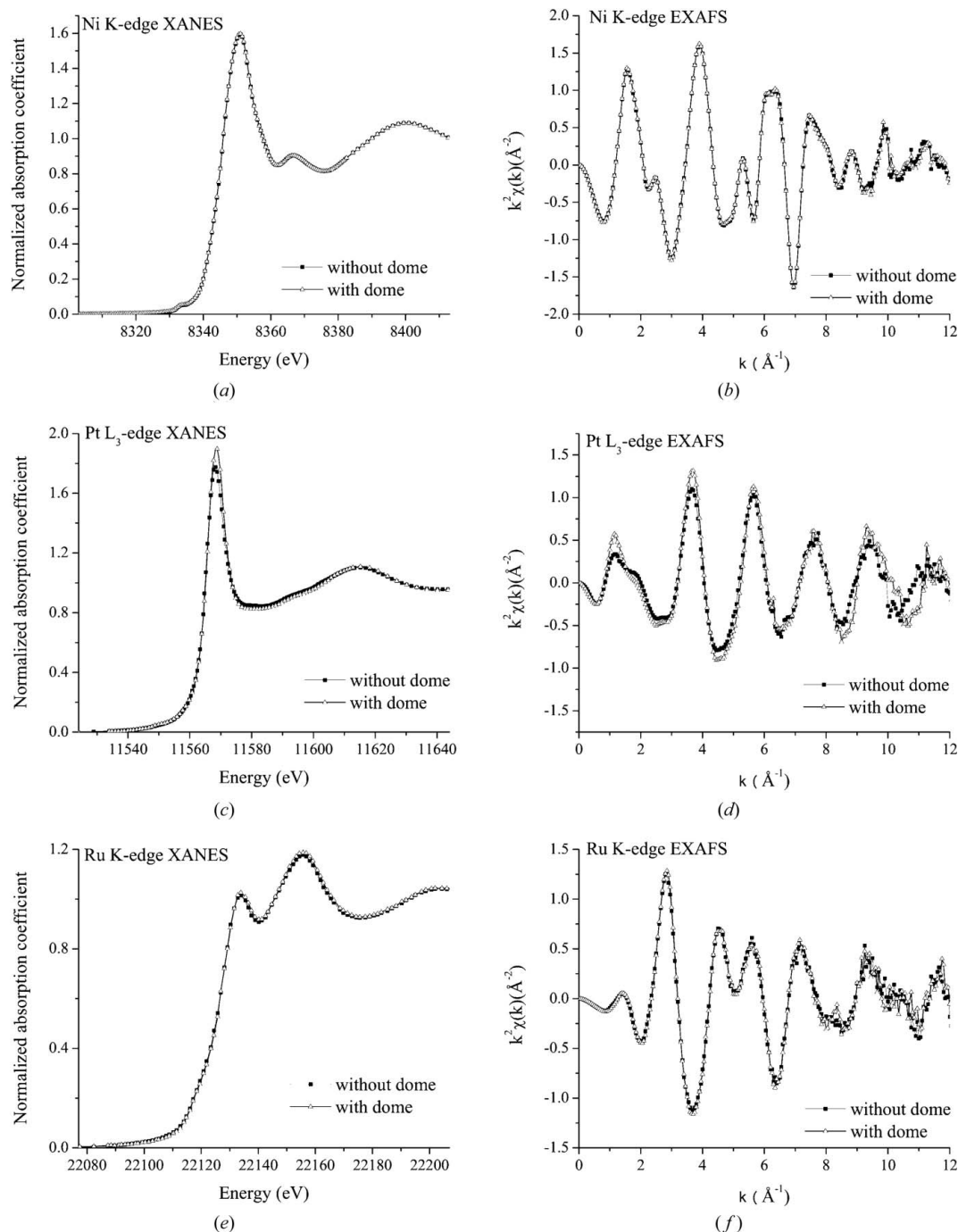


**Figure 4** XAS test results for Ni, Pt and Ru samples using the Harrick cell, with the dome in place (gray lines) and without the dome (black). Normalized absorption  $\mu(E)$  XANES (a, c, e) and  $k^2$ -weighted Fourier transformed EXAFS data (b, d, f) of the Ni K-edge from 4 wt% Ni/Al<sub>2</sub>O<sub>3</sub> (a, b), the L<sub>3</sub>-edge from 1 wt% Pt/Al<sub>2</sub>O<sub>3</sub> (c, d), and the Ru K-edge from 6 wt% Ru<sub>3</sub>(CO)<sub>12</sub>/Al<sub>2</sub>O<sub>3</sub> (e, f). Single XAS scans were taken in normal mode of operation.

that the reduction of Pt commences as soon as CO is introduced, and continues at temperatures below 323 K, as indicated by the decrease in the white line intensity of the Pt L<sub>3</sub>-edge (Fig. 6b). In summary of the XAS data, the two atmospheres (H<sub>2</sub> and CO) affected the Pt white line similarly to what was previously described in the literature (Safonova *et al.*, 2006).

The DRIFT spectra (Fig. 6a) contain several bands at 1700–2300 cm<sup>-1</sup>. The most pronounced is the band around

2080 cm<sup>-1</sup> with a shoulder around 2050 cm<sup>-1</sup>. These bands are ascribed to the linearly bonded CO on the Pt surface (CO<sub>L</sub>) at terrace and step sites, respectively (Lundwall *et al.*, 2010). In addition, two other bands positioned on either side of the CO<sub>L</sub> are also observed. On the higher-frequency side of the CO<sub>L</sub> a band around 2150 cm<sup>-1</sup> is ascribed to the gaseous CO (Primet *et al.*, 1973; Mahan & Lucas, 1978). On the lower-frequency side the band around 1850 cm<sup>-1</sup> is ascribed to the bridged carbon monoxide CO<sub>B</sub>. All these bands reach a maximum in

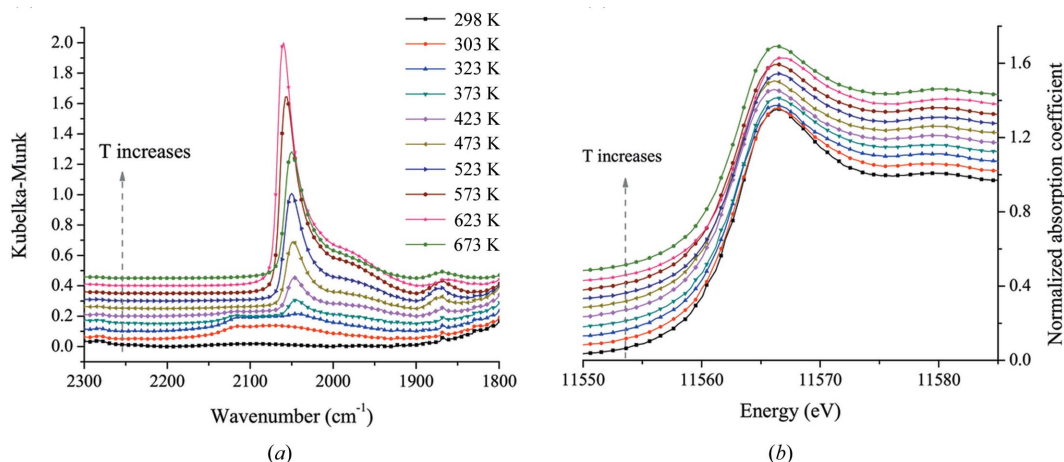


**Figure 5**  
 (a) DRIFTS and (b) Pt  $L_3$  XANES spectra during the reduction of the 5 wt% Pt/ $\text{Al}_2\text{O}_3$  catalyst in 5%  $\text{H}_2/\text{He}$  from room temperature to 673 K. Collection conditions for DRIFTS are identical to that in Fig. 3.

intensity around 323 K. This is accompanied by a frequency shift of the bands to higher wavenumbers. The shift of CO frequency has been observed earlier and explained in terms of the coverage dependence (Eichens & Pliskin, 1958; Blyholder, 1964, 1975; Hammaker *et al.*, 1965; Mahan & Lucas, 1978). Hence, the maximal coverage of the Pt surface with CO is

reached at 323 K in the test experiments. A further increase in temperature causes partial desorption of the CO, observed by the decrease in intensity of the bands ascribed to  $\text{CO}_L$  and  $\text{CO}_B$  and their shift to lower frequencies.

Upon cooling down from 473 K to room temperature in CO atmosphere the IR adsorption bands again start to increase

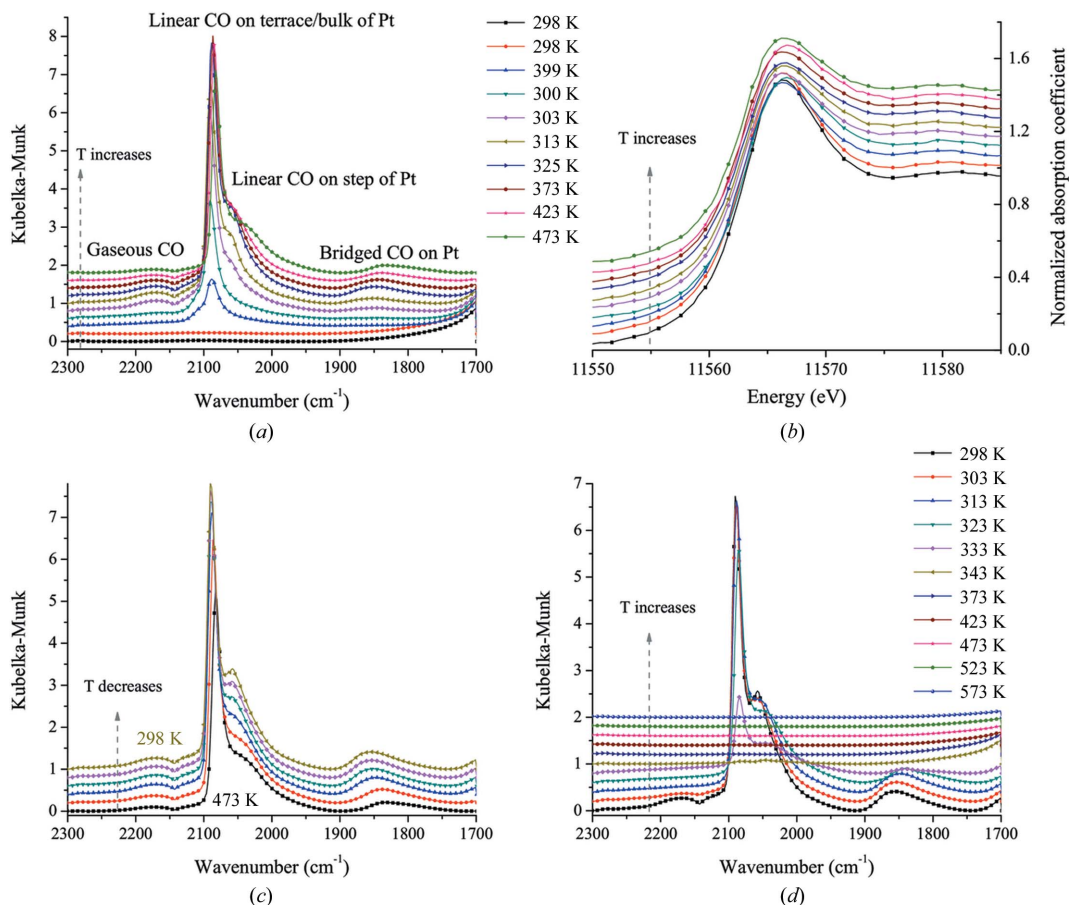


**Figure 6**  
 (a, c, d) DRIFTS and (b) Pt  $L_3$  XANES spectra collected during the CO adsorption in 5%  $\text{CO}/\text{He}$  atmosphere (a, b, c), and CO desorption in He atmosphere (d) on 5 wt% Pt/ $\text{Al}_2\text{O}_3$ . Collection conditions for DRIFTS are identical to that in Fig. 3.

and shift to higher frequencies, as expected upon the increase in CO coverage (Fig. 6c). Once the CO gas has been replaced with He at room temperature, the IR band ascribed to gaseous CO at  $2150\text{ cm}^{-1}$  disappears, whereas the adsorption bands for linear and bridge-bonded CO are still visible (Fig. 6d). As the temperature increases, however, the bands quickly diminish and completely disappear from the spectra at temperatures as low as 333 and 373 K for bridge- and linear-bonded CO, respectively.

### 4. Discussion

The new instrument for collecting *in situ* simultaneous measurements of XAS and DRIFTS offers the following capabilities:

(i) The set-up is installed at the focusing beamline with the beam spot size matching the aperture of the sample cell. It is optimized for energy-scanning XAS measurement mode, including QEXAFS.

(ii) The set-up includes a motorized stage for precise sample alignment and is completely portable. It can be transferred to the NSLS-II light source when it is completed. The focused beam with the higher flux in the broader energy range at the NSLS-II will be crucial for fast scanning times and will enable QEXAFS operations for low catalyst loadings in transmission and/or fluorescence mode.

(iii) The dry-nitrogen purging of the IR spectrometer and the entire IR beam pathway from the IR source to the detector, including DRIFTS accessory optics, allows greater signal-to-noise ratio in those parts of the IR spectrum that are generally masked by the strong stretching bands of  $\text{CO}_2$  ( $2300\text{--}2400\text{ cm}^{-1}$ ), and rotational bands of water vapor ( $3000\text{--}3600$ ,  $1800\text{--}1400$  and  $900\text{--}300\text{ cm}^{-1}$ ). This is particularly important for investigations of catalysts that show metal-adsorbate IR bands in the region below  $1000\text{ cm}^{-1}$ .

This instrument, while fully operational, will require further upgrades. First, the existing geometry of the sample cup does not allow accounting for a wide range of X-ray absorption lengths which are unique for each sample. The cup diameter is currently constant and relatively large ( $\sim 3.2\text{ mm}$ ). The X-ray path length, therefore, in most cases exceeds one absorption length of X-rays in the wide energy range unless the X-ray absorbing material is loaded in a very light matrix. That condition limits the investigations to a very small number of systems, *e.g.* Ag, Pd, Rh, Mo, Ru on alumina or carbon supports, and excludes lighter elements on more absorbing supports (*e.g.* Pt, Au, Ni or Fe on titania or zirconia). One solution is to design and use variable size sample cups that can be inserted in the XAS/DRIFTS cell. One such insert, in the shape of two coaxial cylinders, wider on the top (for IR) and narrower on the bottom (for X-rays), with an X-ray path length of  $\sim 2.2\text{ mm}$ , was used in the test experiments described above, showing that the cell, with such a modification, can be used for a large variety of X-ray energies. However, further studies are necessary to establish the appropriate X-ray path length and cup diameter for various catalysts and their matrices. Another solution is to adapt the existing cell for

fluorescence measurements, in addition to transmission. The latter possibility will be particularly useful for dilute catalyst loadings, which cannot be analyzed by XAS in transmission mode.

Second, the large volume of the existing reactor chamber produces dead-time (*i.e.* the time it takes to replace the entire volume of the cell with a new gas) of the order of 20 s with the existing mass flow controllers (MFCs). Faster MFCs can bring the dead-time to the order of 10 s, which is comparable with the time required to produce good quality spectra in both QEXAFS and rapid-scan DRIFTS regimes. Finally, this set-up is designed for simultaneous X-ray absorption and DRIFT spectroscopy measurements only. However, with some modifications it may be possible to implement other detection modes and/or other techniques. For instance, with a proper modification of the attachment, *e.g.* by redesigning the Praying Mantis mirrors in the DRIFTS accessory and the sample dome, it may be possible to adapt the accessory to detect the X-ray fluorescence. In addition, a similar modification of the DRIFTS accessory may open the possibility of simultaneous *in situ* XRD, in particular, high-energy XRD/PDF measurements together with IR.

### 5. Conclusions

The combination of IR and X-ray absorption spectroscopies in a single experiment provides a fast and reliable analytical method for solving structural and kinetic problems of interest to catalytic science. We described new research capabilities at the NSLS beamline X18A for catalysis research, ones that employ a versatile instrument for *in situ* investigation of a broad range of metals by complementary absorption and vibrational spectroscopies. These two techniques are bulk- and surface-sensitive, respectively. Owing to the time resolution afforded by the QEXAFS capability at the beamline and the fast response of the IR detectors and gas-analysis system, X-ray and IR spectroscopy data collection of the order of tens of seconds under *in situ* conditions are now possible. Selected measurements presented here demonstrate that both IR and XAS techniques operate in a broad range of energies of interest in catalysis science.

We would like to acknowledge the support of the US Department of Energy Grant No. DE-FG02-05ER15688 that supports Synchrotron Catalysis Consortium. We are grateful to the staff of Harrick Co. for many useful discussions and for the design and manufacturing the the DRIFTS assembly. We are indebted to A. Lenhard for manufacturing the positioning table. We thank M. Newton, J. Hanson, J. Rodriguez, R. Nuzzo and R. Adzic for useful discussions, and S. Ehrlich for assistance in beamline tests. We would like to thank L. Barriopliego and C. Cooper for help in beamline experiments. The 1% Pt/ $\text{Al}_2\text{O}_3$  and 16% Ni/ $\text{Al}_2\text{O}_3$  samples were provided by M. Small and J.-Q. Wang, respectively. The National Synchrotron Light Source is supported by the US DOE Grant No. DE-AC02-98CH10886.

## References

- Beale, A. M. & Sankar, G. (2002). *J. Mater. Chem.* **12**, 3064–3072.
- Benitez, J. J., Carrizosa, I. & Odriozola, J. A. (1993). *Appl. Spectrosc.* **47**, 1760–1766.
- Blyholder, G. (1964). *J. Phys. Chem.* **68**, 2772–2777.
- Blyholder, G. J. (1975). *J. Phys. Chem.* **79**, 756–761.
- Brown, M., Peierls, R. E. & Stern, E. A. (1977). *Phys. Rev. B*, **15**, 738–744.
- Brückner, A. (2001). *Chem. Commun.* pp. 2122–2123.
- Chang, J.-R. & Chang, S.-L. (1998). *J. Catal.* **176**, 42–51.
- Clausen, B. S. (1998). *Catal. Today*, **39**, 293–296.
- Clausen, B. S. & Topsøe, H. (1994). *Synchrotron Radiat. News*, **7**, 32.
- Clausen, B. S., Topsøe, H. & Frahm, R. (1998). *Adv. Catal.* **42**, 315–344.
- Eichens, R. P. & Pliskin, W. A. (1958). *Adv. Catal. Relat. Subj.* **10**, 1.
- Estrella, M., Barrio, L., Zhou, G., Wang, X., Wang, Q., Wen, W., Hanson, J. C., Frenkel, A. I. & Rodriguez, J. (2009). *J. Phys. Chem. C*, **113**, 14411–14417.
- Evans, J., Dent, A. J., Diaz-Moreno, S., Fiddy, S. G., Jyoti, B., Newton, M. A. & Tromp, M. (2007). *AIP Conf. Proc.* **882**, 603–607.
- Fondeur, F. & Mitchell, B. S. (2000). *Spectrochim. Acta A*, **56**, 467–473.
- Frahm, R. (1989). *Rev. Sci. Instrum.* **60**, 2515.
- Frenkel, A. I., Kleinfeld, O., Wasserman, S. & Sagi, I. (2002). *J. Chem. Phys.* **116**, 9449.
- Fuller, M. P. & Griffiths, P. R. (1980). *Appl. Spectrosc.* **34**, 533–539.
- Goodwin, J. G. & Naccache, C. (1982). *J. Mol. Catal.* **14**, 259–264.
- Gottschalk, D., Hinson, E. A., Baird, A. S., Kitts, H. L. & Layman, K. A. (2010). *J. Phys. Chem. C*, **114**, 4950–4960.
- Griffiths, P. & de Haseth, J. A. (2007). *Fourier Transform Infrared Spectrometry*. New York: Wiley.
- Grunwaldt, J. D. & Baiker, A. (2005). *Phys. Chem. Chem. Phys.* **7**, 3526–3539.
- Grunwaldt, J.-D. & Clausen, B. (2002). *Top. Catal.* **18**, 37–43.
- Hagelstein, M., Ferrero, C., Sanchez del Rio, M., Hatje, U., Ressler, T. & Metz, W. (1995). *Physica B*, **208/209**, 223–224.
- Hammaker, R. M., Francis, S. A. & Eischens, R. P. (1965). *Spectrochim. Acta*, **21**, 1295–1309.
- Khalid, S. *et al.* (2010). *Rev. Sci. Instrum.* **81**, 015105.
- Klasovsky, F., Hohmeyer, J., Bruckner, A., Bonifer, M., Arras, J., Steffan, M., Lucas, M., Radnik, J., Roth, C. & Claus, P. (2008). *J. Phys. Chem. C*, **112**, 19555–19559.
- Liu, D., Que, G.-H., Wang, Z.-X. & Yan, Z.-F. (2001). *Catal. Today*, **68**, 155–160.
- Lu, S., Lonergan, W. W., Bosco, J. P., Wang, S., Zhu, Y., Xie, Y. & Chen, J. G. (2008). *J. Catal.* **259**, 260–268.
- Lundwall, M. J., McClure, S. M. & Goodman, D. W. (2010). *J. Phys. Chem. C*, **114**, 7904–7912.
- Mahan, G. D. & Lucas, A. A. (1978). *J. Chem. Phys.* **68**, 1344.
- Newton, M. A. (2009). *Top. Catal.* **52**, 1410–1424.
- Newton, M. A., Belver-Coldeira, C., Martinez-Arias, A. & Fernandez-Garcia, M. (2007). *Nat. Mater.* **6**, 528–532.
- Newton, M. A., Dent, A. J., Fiddy, S. G., Jyoti, B. & Evans, J. (2007a). *Catal. Today*, **126**, 64–72.
- Newton, M. A., Dent, A. J., Fiddy, S. G., Jyoti, B. & Evans, J. (2007b). *Phys. Chem. Chem. Phys.* **9**, 246–249.
- Newton, M. A., Jyoti, B., Dent, A. J., Fiddy, S. G. & Evans, J. (2004). *Chem. Commun.* pp. 2382–2383.
- Primet, M. (1984). *J. Catal.* **88**, 273–282.
- Primet, M., Basset, J. M., Mathieu, M. V. & Prettre, M. (1973). *J. Catal.* **29**, 213–223.
- Queau, R. & Poilblanc, R. (1972). *J. Catal.* **27**, 200–206.
- Safonova, O. V., Tromp, M., van Bokhoven, J. A., de Groot, F. M., Evans, J. & Glatzel, P. (2006). *J. Phys. Chem. B*, **110**, 16162–16164.
- So, I., Siddons, D., Caliebe, W. & Khalid, S. (2007). *Nucl. Instrum. Methods Phys. Res. A*, **582**, 190–192.
- Somorjai, G. A. & Aliaga, C. (2010). *Langmuir*, **26**, 16190–16203.
- Szilagyi, T. (1990). *J. Catal.* **121**, 223–227.
- Tinnemans, S. J. *et al.* (2006). *Catal. Today*, **113**, 3–15.
- Wang, Q., Hanson, J. C. & Frenkel, A. I. (2008). *J. Chem. Phys.* **129**, 234502.
- Weckhuysen, B. (2002). *Chem. Commun.* p. 97.